

# Method to Enhance the Frequency Readability for Detecting Incipient Structural Damage

G. R. Gillich<sup>1</sup> · I. C. Mituletu<sup>1</sup> · Z. I. Praisach<sup>1</sup> · I. Negru<sup>1</sup> · M. Tufoi<sup>1</sup>

Received: 2 February 2015 / Accepted: 26 July 2016 / Published online: 17 November 2016  
© Shiraz University 2016

**Abstract** Vibration-based damage detection methods able to recognize cracks in the early state require accurate frequency evaluation in order to identify small modal changes. Because of higher order, the natural frequencies are rapidly damped, time history provides insufficient information if standard frequency estimations are performed. This paper introduces a method of overlaying multiple spectra achieved by iterative truncation of the original signal. In this way, the spectral bin number becomes much higher and the identification of real natural frequencies is easier. Also, an original damage detection algorithm based on the frequency shift is described that considers the first six bending vibration modes occurred due to damage. These are in direct relation to the modal strain energy stored at the damage location. The effectiveness of the detection method is proved using real structures in some damage scenarios. Thus, it was shown that even if a crack reduces the beam's transversal cross section by only 6%, it can be clearly detected.

**Keywords** Cantilever beam · Damage detection · Frequency evaluation · Modal analysis · Overlapped spectrum

## 1 Introduction

Assessment of structural damages can be performed using some global methods of nondestructive evaluation (Abdollahifar and Nami 2014; Arvin 2014). They are based on detecting and analyzing the occurrence of changes in modal parameters. In the case of small damages (Nami and Janghorban 2015), modal parameter values show low-variation and, therefore, the accuracy of frequency evaluation becomes very important in the field of vibration-based damage detection or structural condition monitoring.

Among all damage detection methods, one is more common and is based on the changes given by the natural frequencies. This detection method has a notable advantage, the easy and quick measurement of frequencies. However, for small damages, or in early stages when the detection of damage is more favorable and has the biggest technical and financial advantage, most researchers observed low-variation in frequency values (Sinou 2009).

The minimum amount of damage necessary for a successful detection is determined by an investigation in Richardson and Mannan (1993). Here, the main parameters that influence the prediction are given, these are the number of vibration modes and the errors resulted from measurements. This observation can be assumed for all the vibration-based damage detection methods, overcoming the involvement of modal parameters and the analysis technique. In conclusion, to perform early recognition on the damaged structures, there are two ways to significantly augment the performance of global evaluation methods.

---

✉ G. R. Gillich  
gr.gillich@uem.ro

I. C. Mituletu  
i.mituletu@uem.ro

Z. I. Praisach  
zpraisach@yahoo.com

I. Negru  
i.negru@uem.com

M. Tufoi  
m.tufoi@uem.ro

<sup>1</sup> Department of Mechanical Engineering, "Eftimie Murgu" University of Resita, P-ta Traian Vuia 1-4, 320085 Resita, Romania

The frequency evaluation accuracy is mostly linked to the measurement equipment and technique, limiting the vibration modes number involved in the detection process. Thus, a higher number of vibration modes required by the detection process determines an extended frequency spectrum, causing important problems in fast and accurate frequency evaluation (e.g., the ratio between the tenth transverse vibration mode and its first vibration mode is higher than 300 for a straight cantilever beam).

Especially at higher modes, the free vibration of a structure is quite rapidly damped (Gillich et al. 2012). Therefore, in order to ascertain an adequate frequency resolution, the signal acquisition should be balanced with the acquisition time and the sampling strategy. The resulted resolution is sometimes gross, making early recognition of the damage impossible. Thus, certain doubts with regard to the frequency-based damage detection methods rise up, due to the impossibility of determining small structural cracks or early damaged structures.

Based on what is presented above, the accurate frequency evaluation is imposed as determinative for effective damage detection. Commonly, the frequency spectrum is achieved by applying the Fourier Transform to convert the time-domain signal in the frequency domain. In the literature, two frequency evaluation techniques are often proposed for improving the frequency readability. One of the most frequently used is the zero padding procedure, which is described by Gustafsson et al. (2010). Accentuated important aspects in applications are based on simulated and real data sets.

The Phase-Rotation Fourier Transform (PFT) is introduced as a discrete Fourier transform (DFT) technique by the Böhm et al. PFT increases the spectral information extracted from a data set more than a conventional DFT. Thus, between the spectral bins of DFT more information is obtained, in this way a more accurate amplitude and phase of Fourier components is determined (Böhm et al. 2009).

Jacobsen and Kootsookos (2007) presented a simple computational algorithm that can achieve substantial refinement with regard to the frequency estimation of sinusoidal components. The idea was to estimate the frequency of the peak via a cross-curve, which goes through three neighbor DFT samples. This method is simple and the precision of frequency evaluation is high enough.

The goal of the present paper is to introduce a complete procedure that enhances the accuracy of frequency identification, allowing a more precise evaluation of the natural frequencies. The identification method is based on iterative truncation of the original vibration signal by performing rectangular windowing of different lengths. Afterward, for each truncated time signal a Power Spectral Density (PSD) analysis was applied. Once spectra resulted, they are overlaid in one spectrum, which shows an importantly

increased number of spectral bins. This enhanced spectrum provides an inconstant resolution, but much higher than a classical one. The results are processed, in concordance to an original damage assessment method in order to find the damage location and depth. An important issue is to make the difference between changes determined by damage or by environmental or operational loads, the last ones being sometimes more important. As an example to illustrate how the thermal variation affects the changing of natural frequency values and the way of correcting these values to bring them to the value achieved by a reference temperature is presented in Sect. 2. The advanced frequency estimation method in conjunction with the proposed damage assessment method gives a model of analyzing the frequency shifts due to a crack for multiple weak-axis bending vibration modes. Together, they allow early recognition of small cracks and accurate evaluation of their position.

## 2 Theoretical Background

### 2.1 Thermal Effect on Natural Frequency Values of Beams

The effect of temperature changes is very important, determining different shifts in the dynamic behavior of beams by altering the modal parameters. Therefore, here a model of natural frequencies variation in relation to temperature values is presented. It allows the computation of natural frequencies at any temperature value, providing the possibility to compare these values to those achieved from numerical simulation or real experiments.

Modal shifts appear because the mechanical parameters change, especially when axial loads occur due to constrained beam boundaries. In damage detection this affects the model correctness and can indicate false alarms. The effect of changes in mechanical properties is largely treated in the literature (Deraemaeker et al. 2006; Azadi 2011). In this section, the effect of axial forces induced by the temperature change is analyzed on a clamped–clamped beam. Taking the example of a beam of length  $L$ , width  $b$  and height  $h$ , mass density  $\rho$ , because of the increase or decrease in temperature  $\Delta T$ , achieved from the reference temperature  $T_{\text{ref}}$  to the temperature  $T$ , an internal load  $P$  occurs. It can be expressed as Tufoi et al. (2014):

$$P(T) = \alpha \cdot E \cdot b \cdot h \cdot \Delta T = \alpha \cdot E \cdot b \cdot h \cdot (T - T_{\text{ref}}) \quad (1)$$

In relation (1)  $E$  is denoted the longitudinal elastic modulus and  $\alpha$  thermal expansion coefficient.

Because of buckling, the beam deforms:

$$EI \frac{d^2 v}{dx^2} + Pv = 0 \Leftrightarrow \frac{d^2 v}{dx^2} + \zeta^2 v = 0, \quad \zeta^2 = \frac{P}{EI} \quad (2)$$

where  $I$  is a second moment of inertia. The solution of this equation is given by:

$$v(x) = c_1 \sin(\zeta x) + c_2 \cos(\zeta x) + c_3 x + c_4 \tag{3}$$

In prior research, we demonstrated (Gillich and Praisach 2012) that the natural frequency value of a beam with an open crack  $f_{iD}(p, d)$  of depth  $d$  and located at distance  $p$ , is:

$$f_{iD}(p, d) = f_i \left( 1 - \gamma(d) (\bar{\phi}_i''(p))^2 \right) \tag{4}$$

Thus, it is possible to predict the natural frequency values of a beam with known damage configuration, for any temperature lower than a critical value  $T_{cr}$  for which the buckling effect arises as:

$$\begin{aligned} f_{iD}(p, d, T) &= f_i(T) \left( 1 - \gamma(d) (\bar{\phi}_i''(p))^2 \right) \\ &= f_{i\_ref} \left( 1 - \gamma(d) (\bar{\phi}_i''(p))^2 \right) \sqrt{1 - \frac{\alpha \Delta T}{R_g^2} \left( \frac{L^2}{\zeta_i^2} \right)} \end{aligned} \tag{5}$$

where  $\gamma(d)$  reflects the damage severity and  $\bar{\phi}_i''(p)$  is the normalized mode shape curvature at location  $p$  for the  $i$ -th weak-axes bending vibration (Tufoi et al. 2014). In a similar way, these frequencies can be determined for any pre-buckling load as:

$$\begin{aligned} f_{iD}(p, d, P) &= f_i(P) \left( 1 - \gamma(d) (\bar{\phi}_i''(p))^2 \right) \\ &= f_{i\_ref} \left( 1 - \gamma(d) (\bar{\phi}_i''(p))^2 \right) \sqrt{1 - \frac{P}{EI} \left( \frac{L^2}{\zeta_1^2} \right)} \end{aligned} \tag{6}$$

Relations (5) and (6) are of great importance as they allow the frequencies accomplishment for undamaged and damaged beams, any temperature or axial load in the pre-buckling domain. Also, they allow the comparison between the frequencies of a beam acquired in the monitoring process to those computed at different temperature values. In a similar way, the effect of other elements producing changing conditions can be suppressed.

### 2.2 Damage Location Assessment by a Frequency-based Method

Frequency-based damage assessment method makes use of the characteristic equation, relating the natural frequencies of the damaged structure to the damage parameters. Let us consider, for simplicity, the assessment process for an invariant environment. In this case, the temperature does not affect the natural frequencies. Thus, relations (5) or (6) become (10):

$$f_{iD}(p, d) = f_{iU} \left( 1 - \gamma(d) \cdot (\bar{\phi}_i''(p))^2 \right) \tag{7}$$

Here,  $f_{iD}(p, d)$  is the natural frequency of the damaged beam,  $p$  crack location,  $d$  depth,  $f_{iU}$  the natural frequency of transverse mode  $i$  in healthy state,  $\gamma(d)$  damage severity,  $\bar{\phi}_i''(p)$  normalized mode shape curvature value in  $p$  for the  $i$ -th vibration mode.

$(\bar{\phi}_i''(p))^2$  was determined in relation to the locally stored energy and the corresponding vibration mode.  $\gamma(d)$  can be achieved by numerical simulations or static measurements of the beam deflection in the undamaged state  $s_U$  and the damaged state  $s_D(d)$ :

$$\gamma(d) = \frac{\sqrt{s_D(d)} - \sqrt{s_U}}{\sqrt{s_D(d)}} \tag{8}$$

Damage severity reflects the increasing global beam stiffness (Praisach et al. 2013). Equation (7) provides right values for any beam support types and all cross section shapes, resulting the frequency shift due to the crack:

$$\Delta f_i(p, d) = f_{iU} - f_{iD}(p, d) = f_{iU} \cdot \gamma(d) \cdot (\bar{\phi}_i''(p))^2 \tag{9}$$

Frequency shift  $\Delta f_i$  normalized by the frequency of healthy beam  $f_{i-U}$  leads to the relative frequency shift accomplishment for any bending vibration mode  $i$ :

$$\Delta \bar{f}_i(p, d) = \gamma(d) \cdot (\bar{\phi}_i''(p))^2 \tag{10}$$

Some two-dimensional and three-dimensional typical curves of frequency shift are presented in Gillich et al. (2012, 2014), Gillich and Praisach (2014) for several beam types. Frequency shifts for a single damage severity are two-dimensionally represented, and those considering severities continuously distributed along the range of possible values are three-dimensionally illustrated. Comparable graphical representations have been found, and they also show accomplishments achieved either by laborious calculations (Afshari and Inman 2013; Khiem and Toan 2014) or curve fitting (Ekinovic 2010). The methods involved require extended calculation and/or many experimental results, in order to achieve adequate characteristics, perform sequential analysis for each individual damage case, and consider the location and severity. On the contrary, using Eq. (10) leads to the determination of frequency shift values for all types of beam, damage location and severity.

In the general case, a pattern consisting of relative frequency shift values of several modes (in form of a sequence), corresponding to a crack of depth  $d$  located at distance  $\delta = p/l$  from the beam end, has the following expression:

$$\Delta \bar{f}_i(\delta, d) = \gamma(d) \cdot (\bar{\phi}_i''(\delta))^2 \tag{11}$$

The effect of damage depth for individual parameters  $\Delta \bar{f}_i(\delta, d)$  can be canceled, if they are divided to the highest

value of the series, accomplishing in the same time the normalization of relative frequency shift values for each location  $p$ . In this way, the series of values becomes independent of the damage severity, its parameters taking values between 0 and 1. The series has been called *Damage Location Indicators* (DLI) and the individual parameters *Damage Location Coefficients* (DLC):

$$\phi_i(\delta) = \frac{(\bar{\phi}_i''(\delta))^2}{\max\{(\bar{\phi}_1''(\delta))^2 \dots (\bar{\phi}_n''(\delta))^2\}} \quad (12)$$

An important note, DLCs can be achieved by only collecting information about the beam's healthy state. Another important thing, DLCs uniquely characterize locations on asymmetric structures. In the symmetric case, two mirrored locations employ the same value of DLC.

Supposing  $f_{iU}^m$  and  $f_{iD}^m$  the  $i$ -th natural frequency in the weak-axis bending vibration modes measured on a beam in healthy state or damaged, the relative frequency shifts:

$$\Delta \bar{f}_i^m = \frac{f_{iU}^m - f_{iD}^m}{f_{iU}^m} \quad (13)$$

By normalization, the accomplished dimensionless values are severity-independent (Gillich et al. 2014). The individual parameters are denoted as *Measured Normalized Frequency Shifts* and the entire  $\psi$  sequence as *Damage Signature* (DS):

$$\Psi_i = \frac{\Delta \bar{f}_i^m}{\max\{\Delta \bar{f}_1^m \dots \Delta \bar{f}_n^m\}} \quad (14)$$

Thus, these parameters are assumed as having a meaning similar to the DLCs.

Considering that any damage has a DS associated, determined by measurements, and a certain number of damage locations  $u$  equidistantly positioned along the beam; it is possible to determine DLIs as  $\Phi_j(\delta_j)$ ,  $j$  taking values from 1 to  $u$ . Pair vectors can be determined by associating *Damage Signature*  $\psi$  to *Damage Location Indicators*  $\Phi_j$ . So that DLIs indicate damage locations  $\delta_j$ . Location precision is improved by increasing the number of considered locations  $u$ . More exact position (error  $<1\%$ ) is achieved for  $u = 100$ . To determine the most similar vectors, the Minkowski distance of second order is involved:

$$DI_j = \left( \sum_{i=1}^n |\Phi_i(\delta_j) - \Psi_i|^2 \right)^{\frac{1}{2}} \quad (15)$$

Actually, the goal is to determine the value of  $j$ , where function  $DI_j$  reaches the lowest value, indicating the crack location  $\delta_j$ . In this regard, an identification algorithm is presented below:

- in the initial, supposed healthy state, a frequency evaluation is performed to achieve the first  $n$  weak-axis bending vibration modes (for more precision  $n$  is recommended between 6 and 10). Here  $n = 6$ , resulting in  $f_{n-U}^m$ -series;
- for each investigated moment, the frequencies of vibration modes must be periodically evaluated, achieving  $f_{n-D}^m$ -series;
- the frequency shifts are determined by comparing the initial to the actual state. Subtracting the values of step 2 from step 1, we have  $\Delta f_n^m$ -series. If the difference is quite insignificant ( $<1\%$ ) and similar for all modes, the structure is healthy, and otherwise it is damaged.
- if damage is suspected, relative frequency shifts are computed  $\Delta \bar{f}_n^m$ ;
- subsequently, parameters of  $\Delta \bar{f}_n^m$ -series are normalized, resulting in DS as  $\Psi_n$ -series;
- for healthy beam,  $(\bar{\phi}_n''(\delta_p))^2$ -series representing the squared mode shape curvatures are analytically determined for  $p$  locations on the beam;
- by dividing the parameters of  $(\bar{\phi}_n''(\delta_p))^2$ -series to the highest value of the same series, DLIs are resulted  $\Phi_n(\delta_j)$ ;
- resulted  $\Phi_n(\delta_j)$ -series is compared involving Minkowski Distance to the  $\Psi$ -series, determined by measurements to identify the DLI that best fits the DS. Damage location is indicated by  $\delta_j$  coordinate, for which the best fit is achieved.

Considering the beam damaged in the initial state, the identification algorithm shows the damage evolution. Because the superposition principle is applicable in case of multiple cracks, this possibility has to be considered. In Praisach and Gillich (2013) such a demo-case is extensively described. Moreover, if damage patterns are designed for multiple damage scenarios, including many cracks, their assessment can be performed by this method.

### 2.3 Frequency Identification Enhancement

Damage detection methods based on modal analysis employ accurate frequency identification. Where spectra are achieved by common methods, it is almost impossible to identify small frequency variation. Therefore, small cracks or early damage stages can often not be detected. Vibration signals given by healthy or damaged beams are rapidly damped, and the accomplished spectrum density is poor.

Here a method is presented to enhance the frequency identification. The method does an overlaying of multiple spectra, in this way increasing the number of spectral bins. The individual spectra are accomplished by iteratively

windowing the original time signal and afterward performing *Power Spectral Density* (PSD) analysis. The windowing process consists of cropping the original time signal, which is considered through the parameters:  $T_S$ —time length,  $N_S$ —number of samples and  $t_s$ —constant sampling time.

Nyquist theorem gives the spectrum range between 0 and  $f_M$ :

$$f_M = \frac{1}{2t_s} = \frac{N_S - 1}{2T_S} \tag{16}$$

Frequency resolution  $\Delta f$  depends on time length  $T_S$ :

$$\Delta f = \frac{1}{T_S} = \frac{1}{(N_S - 1)t_s} \tag{17}$$

Cropping a number of samples from the original signal, a window with reduced time length  $T_E < T_S$  results. Thus, frequency spectral density  $\Delta f$  decreases with respect to  $T_E$ . Iteratively windowing the original signal and analyzing by PSD at iteration, a number of spectra equal to the number of iterations is achieved. Overlaying all spectra, an overlapped spectrum results that provides much higher spectrum density.

Figure 1 presents the theoretical approach, where:  $S_1, S_2, S_3$  are spectra accomplished by windowing,  $\Delta f_1 < \Delta f_2 < \Delta f_3$  the corresponding frequency resolutions and  $T_1 > T_2 > T_3$  time lengths. Here an inconstant spectral bins distribution is observed, but also a clearly increased spectrum density.

Spectrum of the original signal (red continuous lines) has poor frequency fit, but the spectrum of the second cropped signal (blue dash-dot lines) has a bin that clearly matches the best frequency value. Thus, how a supposed natural frequency can be much easier identified is presented. Obviously, if the sampling rate is higher and more iteration is performed, the spectrum density greatly increases. A comparison with other methods, for instance, as introduced by Jacobsen and Kootsookos (2007) is performed in Minda et al. (2015), clearly demonstrating the higher precision of the method proposed in this paper.

Because a modal analysis requires more than one natural frequency, the procedure has to be repeated for each one,

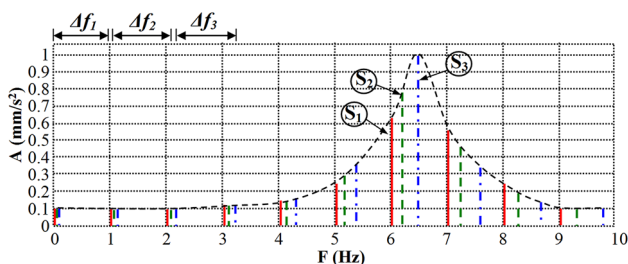


**Fig. 1** Theoretical background for the achievement of the overlapped spectrum

due to the fact that the cropping time portion  $T$  depends on searched frequency  $f_i$ , and implicit of its corresponding time period  $T_{fi}$ :

$$T = (1 \dots 1.3)T_{fi} \tag{18}$$

Also, during this period  $T$  more or less number of samples can be cropped at iteration, resulting in more or less iteration and a corresponding number of spectra, which determine the frequency spectral density (FSD).

Therefore, frequency identification procedure must be performed in four steps:

- iteratively decreasing certain samples number by windowing the original time signal;
- after each windowing, PSD analysis provides a spectrum;
- after iteration, all spectra are overlaying, achieving an overlapped spectrum with high-resolution;
- in the high-resolution spectrum, the searched natural frequency is identified in its area at the maximum amplitude.

This procedure was algorithmically implemented in the LabView as loop-processing structure and the overlapped spectrum has been graphically achieved.

Thus, FSD strictly depends on  $T_S$ —acquisition time length,  $N_S$ —sample number,  $k$ —iteration number and  $q$ —sample number cropped at iteration.

### 3 LabView Implementation of the Frequency Identification Algorithm

The frequency identification algorithm was implemented in LabView as a parameter depending loop-structure. It performs an iterative loop, windowing and analyzes by PSD of the vibration time signal. Then, all the achieved spectra are overlaid and graphically shown in a spectrum.

For a searched natural frequency  $f_i$ , the identification algorithm firstly calculates the  $T$  period, which will be iteratively cropped. Actually, this period consists of  $N_S$  samples. If one sample is cropped at iteration,  $N_S = k$  and an equal number of spectra results. In the case of small frequency value (<25 Hz), not more than  $k = 30$  iterations are needed. Therefore, the algorithm calculates de number of samples cropped at iteration  $q$ :

$$q = \frac{N_S}{k} \tag{19}$$

The number of iterations for some frequency ranges is: 30 for  $0 \rightarrow 25$  Hz, 20 for  $25 \rightarrow 100$  Hz and 10 over 100 Hz. Also, an important aspect has to be highlighted, the higher frequency is searched, the higher sampling rate must taken, because the cropped period becomes shorter. In



fact, the algorithm searches for an integer number of periods corresponding to the searched natural frequency  $f_i$ . In the overlapped spectrum, in the area of this frequency value a lobe formed by many bins is achieved. Frequency best fits in the peak of lobe. In certain situations, this lobe is unclear and does not allow precise frequency identification. Therefore, the lobe area should be cleared of undesired lobe fragments by setting up certain parameters of the algorithm.

The algorithm iteration can start from the last sample of the original signal (taken as the first sample, when the decreasing could begin) or any other sample within the cropped period  $T$ . At the end of period  $T$  is the iteration stop point  $N_{Sp}$ . If the iteration is performed taking the first sample as the start point ( $N_{St}$ ), many superposed spectra are accomplished and the requested frequency could be difficult to distinguish due to repetitive lobe superposition. To avoid such tangled behavior,  $N_{St}$  has to be set so a single and clear peak of lobe can be achieved.

Figure 2 shows the window tuning of a given time signal, indicating the point of: first sample in (1),  $N_{St}$  in (2) and  $N_{Sp}$  at the end of  $T$  (3).

This example is considered to check the algorithm efficiency. Set values for all the involved parameters are given in Table 1. They are specified in case of two mixed frequencies, generated by the LabView, these are 9.12 and 25.3 Hz. The algorithm has to be tuned up for each frequency, so two analyses are requested. The yellow background marks the parameters auto-computed after the algorithm starts.

By performing an analysis and setting the first row of values from Table 1, the image from Fig. 3 has been displayed, indicating the two main lobes at 9.12 and 25.3 Hz. Two dashed cursors precisely indicate both A and B frequencies.

To see more accurate aspects of the peak pointed values, after performing separate analyses for both frequencies,

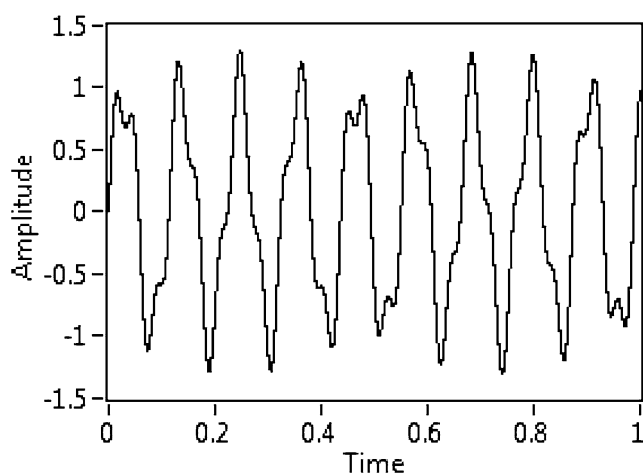


Fig. 2 Cropping scenario for 9.12 Hz

Table 1 Parameters involved into the algorithm

$T_s$ (s)	$N_s$	$t_s$ (s)	$f_i$ (Hz)	$T$ (s)	$N_{St}$	$q$	$N_{Sp}$	$k$
1	50,000	$2 \times 10^{-5}$	9.12	0.1096	3100	80	5480	30
1	50,000	$2 \times 10^{-5}$	25.3	0.0395	20	65	1975	30

Fig. 4 is provided to show the magnified details of both locations.

In the case of 25.3 Hz,  $q$  is differently set in order to rearrange the number of bins in the lobe area. Thus, the density of bins around the peak location is almost the same, see Fig. 4b.

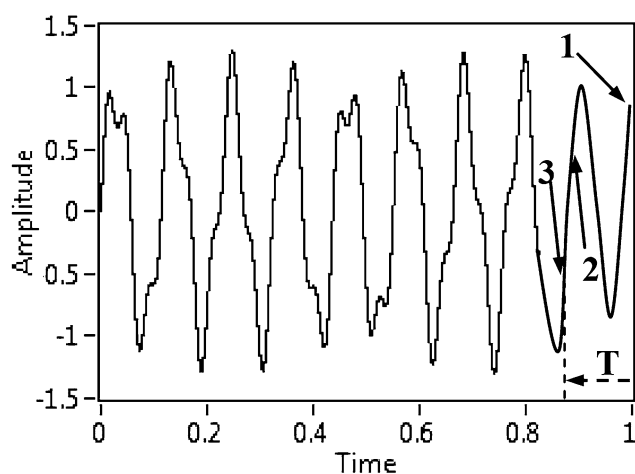
Figure 5 simply indicates for 9.12 Hz how the lobe area has been cleared by the other undesired lobe fragments, performing the  $T$ ,  $q$  and  $N_{Sp}$  setup adequately, Fig. 5b. In Fig. 5a., a greater  $T$  period is taken and therefore the expected lobe is formed but shadowed by others. Also, taking a greater value for  $q$ , the same as in the case of 9.12 Hz, results in the worst case presented in Fig. 5c.

At this point, an important fact has to be noted, once frequency value increases, the sampling rate must be increased in order to get clearer identification. If this is not possible, a spline curve can be plotted through the bins end-points around the estimated peak, and the highest point of it indicates the frequency best fit, as given in Fig. 4.

## 4 Results and Discussion

To prove the effectiveness of the presented method suitable tests have been performed. Tests were accomplished for a clamped-free type cantilever beam defined by the following characteristics given in Table 2.

The parameters from Table 2 mean:  $l$ —beam length,  $w$ —beam width,  $p$ —crack location,  $w_c$ —crack width,  $d$ —



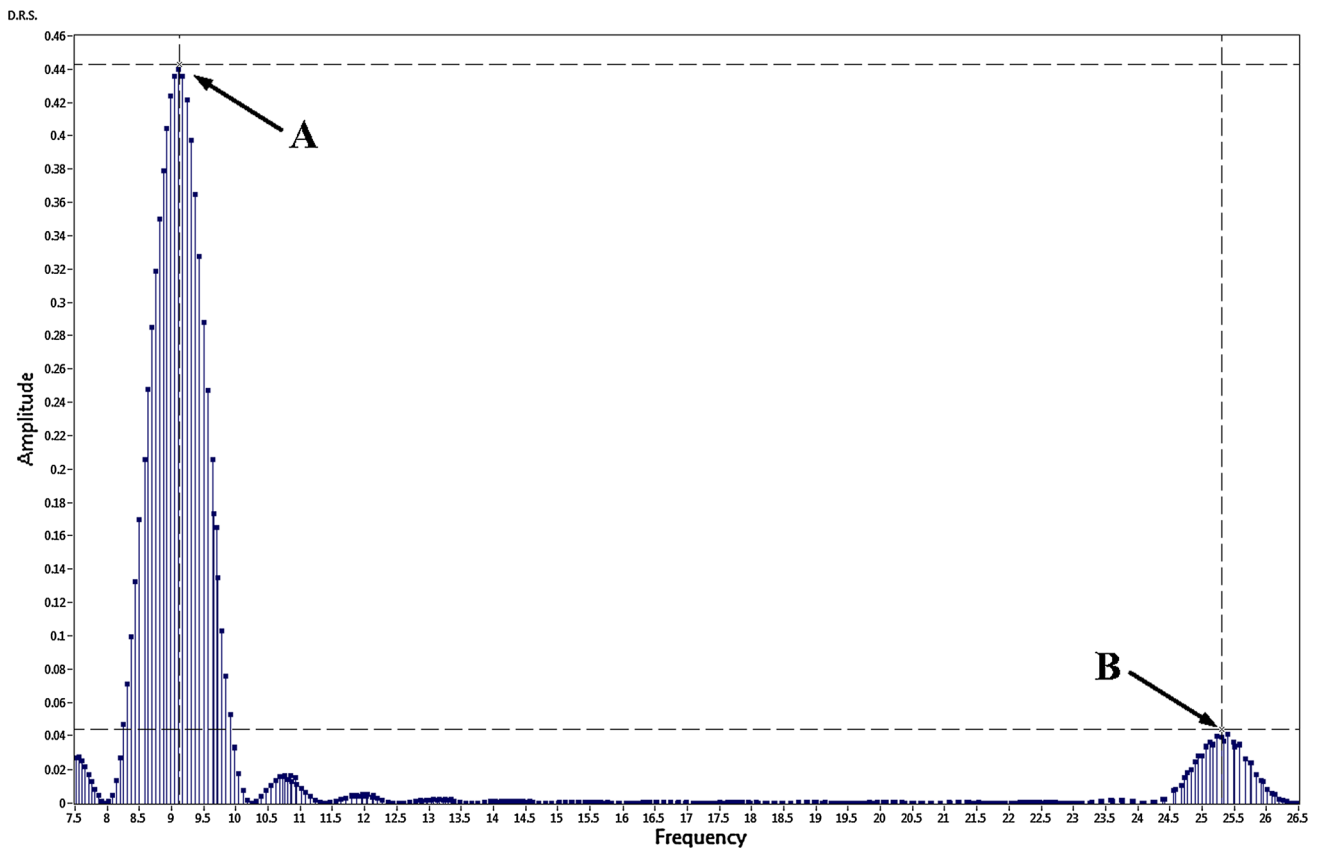


Fig. 3 Lobes formation at 9.12 and 25.3 Hz in the overlapped spectrum

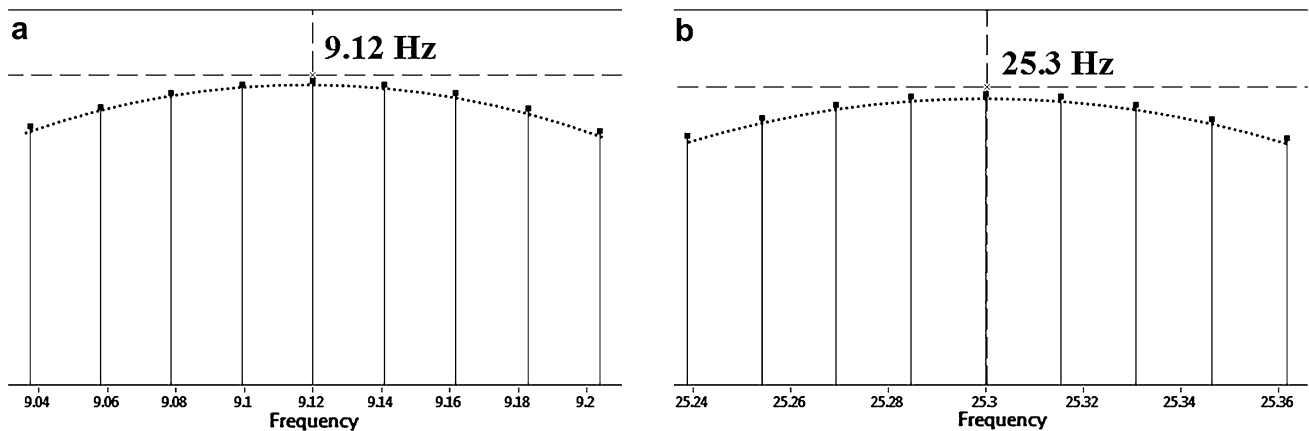


Fig. 4 Zoom areas of both peak lobes after adequately setup

crack depth,  $t$ —beam thickness,  $I$ —moment of inertia,  $\rho$ —mass density,  $E$ —Young’s modulus and  $\mu$ —Poisson’s ratio. The beam was clamped at the left-end by a fixing frame FF.

A three-dimensional schematization of the test stand and the damage location are presented in Fig. 6.

The test stand setup is completed by adequate equipment, which consists of: personal computer, NI cDAQ-9172 chassis, NI 9234 analog-to-digital signal acquisition module and Kistler 8772 three-axial piezoelectric

accelerometer. The accelerometer S is positioned at the free end of the beam. The frequency identification algorithm is a post-processing software procedure performed in LabView, as described in Sect. 3. The setup aims to achieve the first six weak-axis bending vibration modes. Acquisition time was  $t_s = 0.5$  s and the number of samples  $N_s = 50,000$ .

First, by performing an ordinary PSD analysis of the original signal the natural frequencies have been

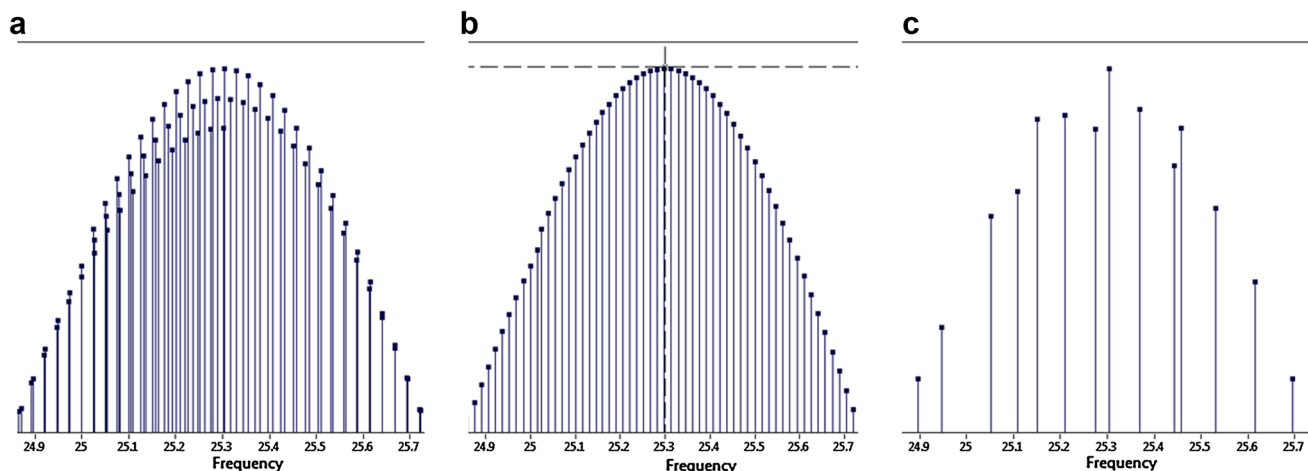
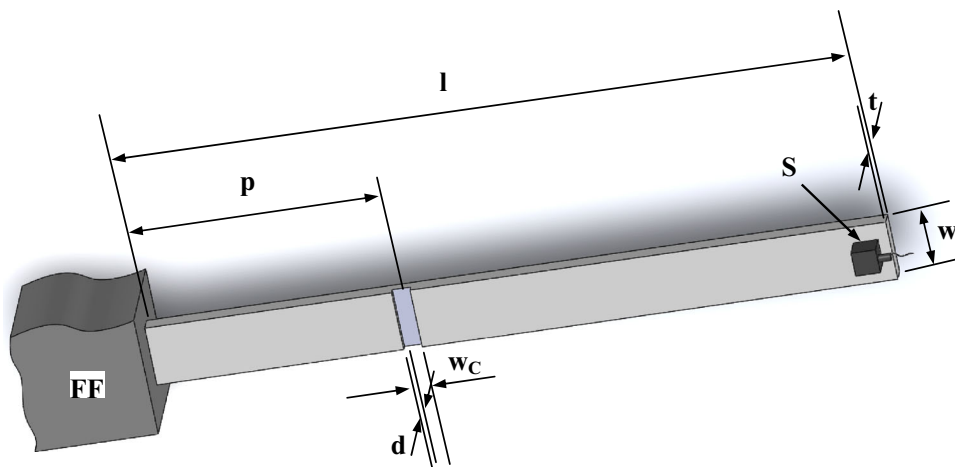


**Fig. 5** Three cases of lobe formation: **a**  $T$  is too big; **b**  $T$ ,  $q$  and  $N_{St}$  have right values; **c**  $T$  is too big and  $q$  is the same as for 9.12 Hz

**Table 2** Characteristics of the cantilever beam

Case	$l$ (mm)	$w$ (mm)	$p$ (mm)	$w_c$ (mm)	$d$ (mm)	$t$ (mm)	$I$ (m <sup>4</sup> )	$\rho$ (kg/m <sup>3</sup> )	$E$ (N/m <sup>2</sup> )	$\mu$ (–)
1	900	50	333	1	0.3	5	$520.833 \times 10^{-12}$	7850	$2.0 \times 10^{11}$	0.3
2	900	50	333	1	0.8	5	$520.833 \times 10^{-12}$	7850	$2.0 \times 10^{11}$	0.3

**Fig. 6** Schematic of the cantilever beam and damage location



experimentally determined. This step provides appreciative values for the natural frequencies. They help to properly setup the frequency identification algorithm. Afterward, the frequency identification algorithm was applied for each natural frequency and for each one it was frequency-dependent setup to precisely identify the real value of natural frequencies.

For the final comparison, three cases have been defined for testing. They were taken in order to easily highlight the precision level of the frequency identification and further on damage detection. Case one assumes a not damaged cantilever beam, the second one provides a 0.3 mm damage depth and the third considers a 0.8 mm depth of crack. The

second crack can be easily assumed as a bigger scratch rather than a considerable damage, due to its so small dimension.

The average of five measurements was considered in each case, just to clarify the differences that should manifest between them. In Table 3, the following parameters are presented for the undamaged beam: AD—absolute difference between the lowest and the highest value of frequency stored for each transversal vibration mode, PD—its percentage conversion and the average of five frequency values achieved at each vibration mode.

Little absolute and percentual differences between the values of frequencies for each mode are determined. They are less than 0.3 in absolute and 0.1% in percentage. These



**Table 3** Accomplishment of the natural frequencies by signal post-processing for the undamaged beam

VM	TN 1	TN 2	TN 3	TN 4	TN 5	AD (Hz)	PD (%)	Average (Hz)
1	5.09574	5.09447	5.09656	5.09473	5.09375	0.0028	0.05499	5.09505
2	31.93546	31.94153	31.93929	31.92492	31.93227	0.01661	0.05199	31.9347
3	89.41741	89.41698	89.40809	89.42966	89.43887	0.03079	0.03442	89.4222
4	175.22244	175.24952	175.08752	175.20667	175.25924	0.17172	0.09798	175.205
5	289.65527	289.72189	289.73058	289.62630	289.60024	0.13034	0.04499	289.667
6	432.69481	432.77703	432.67102	432.52606	432.82462	0.29856	0.06898	432.699

**Table 4** Natural frequency averages,  $DS$ s and  $DLI$ s, for damage positioned at  $p/l = 0.3$

VM	$A_U$ (Hz)	$A_{d1}$ (Hz)	$DS_{d1}$ (-)	$A_{d2}$ (Hz)	$DS_{d2}$ (-)	$DLI$ (-)
1	5.0950493	5.0810535	0.659396	5.064479	0.7425601	0.75744
2	31.934694	31.911872	0.217861	31.87715	0.2150864	0.22207
3	89.422203	89.125553	0.843212	88.76585	0.9486784	0.94128
4	175.20508	175.00378	0.310852	174.7269	0.3257638	0.33634
5	289.66686	289.53776	0.097873	289.3813	0.1101505	0.11754
6	432.69871	431.33261	1	429.2981	1	1

differences are explained by the occurrence of initial phase at different modes and the relative values of acceleration.

In case of usual analysis, no or very poor frequency shifts can be distinguished for a certain vibration mode. Therefore, those poor shifts achieved by post-processing confirm the accuracy and effectiveness of this procedure. It can be concluded that the fine frequency shifts do not depend on the physical phenomenon and cannot be identified in a usual spectrum due to the small number of bins.

$A_U$ , the natural frequency averages are given for the undamaged beam,  $A_{d1}$  is assumed as early damage or incipient states of the damage and  $A_{d2}$  a certain damage progression are presented in Table 4, to more easily compare and conclude where significant frequency shifts occur.

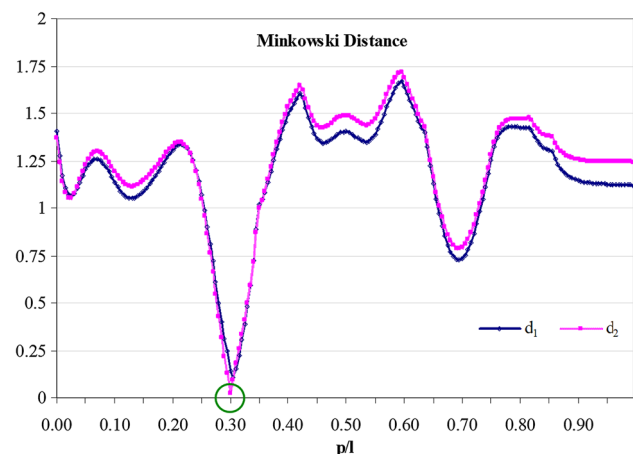


**Fig. 7** Graphical achievement of damage location ( $p/l = 0.3$ ) by performing Minkowski distance

Similar values among  $\Phi_j$  and  $\Psi$  vectors are determined by Minkowski metrics, Fig. 7. The exact location of damage is difficult to detect in its incipient state, considering reduced cross sections less than 6%. But if the damage advances, DS is more clearly obtained and the damage location is easy and offers more accurate data.

The balance between  $DLI$  and  $DS_{d2}$  is presented by green and magenta in Fig. 8, leading to a Minkowski value closed to 0 at damage position. Visible differences occur in mode 1 and 2 for  $DS_{d1}$ ; they are emphasized by blue and green, leading to a bigger Minkowski value and consequently providing less precision.

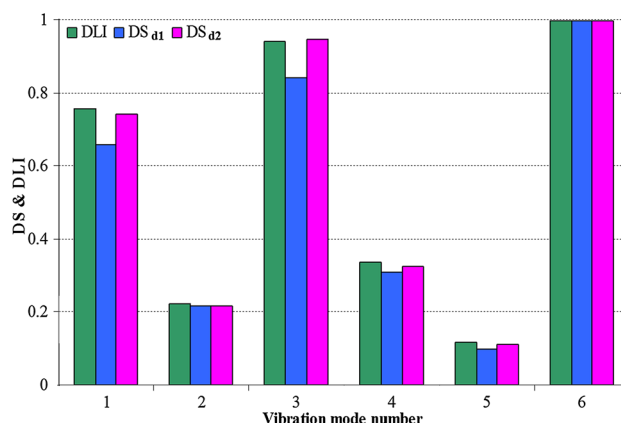


**Fig. 8** Graphical comparison between  $DS$ s and the  $DLI$  shows the precision of damage identification, for location  $p/l = 0.3$

## 5 Conclusion

The paper presents a complete procedure to precisely identify the natural frequencies and to locate the damage, taking as an example the clamped-free cantilever beam. The high grade of accuracy provided by the procedure makes it possible to detect damages in very early stage or small cracks.

This procedure consists of a frequency identification algorithm and a vibration-based damage detection algorithm. If the frequency identification algorithm is properly setup, it provides a dense overlapped spectrum, and clear lobes form in the area of expected natural frequencies. Thus, frequency values can be identified at a high level of precision. The effectiveness of algorithm was tested for theoretical signals as well as for the signals achieved from real experiments.

Adding the precision offered by the frequency identification algorithm to the vibration-based damage detection algorithm, it will finally become possible to accurately indicate the damage location even in very incipient stages, i.e., for reduced cross section of only 6%. In conclusion, this procedure is very sensitive at any kind of transversal crack and for any structure cross section or support type.

The operation of this procedure is complex enough, but it was not designed to require complicated knowledge. Thus, specialists of the area can easily use it having minimum training in working with the mathematical support of the damage detection algorithm, and the technical background needed to properly setup the frequency identification algorithm.

**Acknowledgements** The work has been funded by the Sectoral Operational Programme Human Resources Development 2007–2013 of the Ministry of European Funds through the Financial Agreement POSDRU/159/1.5/S/132395.

## References

- Abdollahifar RA, Nami MR (2014) Determination of dynamic stress intensity factor in FGM plates by MLPG method. *IJST Trans Mech Eng* 38(M1):181–194
- Afshari M, Inman DJ (2013) Continuous crack modeling in piezoelectrically driven vibrations of an Euler-Bernoulli beam. *J Vib Control* 19(3):341–355
- Arvin H (2014) Frequency response analysis of higher order composite sandwich beams with viscoelastic core. *IJST Trans Mech Eng* 38(M1):143–155
- Azadi M (2011) Free and forced vibration analysis of FG beam considering temperature dependency of material properties. *J Mech Sci Technol* 25(1):69–80
- Böhm M, Tasche M, Seifert B, Mitschke F (2009) Trim-to-coherence Fourier transform, Elsevier, ScienceDirect. *J Comput Phys* 228:2906–2917
- Deraemaeker A, Preumont A, Kullaa J (2006) Modeling and removal of environmental effects for vibration based SHM using spatial filtering and factor analysis. In: *Proceedings of IMAC XXIV*. St Louis
- Ekinovic E (2010) An approximate technique for damage identification in beams using shifts in natural frequencies. In: *Proceedings of the 22nd international conference on noise and vibration engineering*, paper 0024
- Gillich GR, Praisach ZI (2012) Damage-patterns-based method to locate discontinuities in beams. In: *Proceedings of SPIE 8695, health monitoring of structural and biological systems*, paper 869532
- Gillich GR, Praisach ZI (2014) Modal identification and damage detection in beam-like structures using the power spectrum and time-frequency analysis. *Signal Process* 96:29–44
- Gillich GR, Praisach ZI, Abdel Wahab M, Vasile O (2014) Localization of transversal cracks in sandwich beams and evaluation of their severity. *Shock Vib* 2014:1–10
- Gillich GR, Praisach ZI, Iavornic CM (2012) Reliable method to detect and assess damages in beams based on frequency changes. In: *Proceedings of the ASME international design engineering technical conferences and computers and information in engineering conference 2012*, vol 1, Pts. A and B. pp 129–137
- Gustafsson F, Ljung L, Millnert M (2010) *Signal processing*. Studentlitteratur, Lund
- Jacobsen E, Kootsookos P (2007) Fast, accurate frequency estimators. *IEEE Signal Process Mag* 24:123–125
- Khiem NT, Toan LK (2014) A novel method for crack detection in beam-like structures by measurements of natural frequencies. *J Sound Vib* 333:4084–4103
- Minda AA, Gillich N, Mituletu IC, Ntakpe JL, Manescu T, Negru I (2015) Accurate frequency evaluation of vibration signals by multi-windowing analysis. *Appl Mech Mater* 801:328–332
- Nami MR, Janghorban M (2015) Free vibration of functionally graded size dependent nanoplates based on second order shear deformation theory using nonlocal elasticity theory. *IJST Trans Mech Eng* 39(M1):15–28
- Praisach ZI, Gillich GR (2013) Influence of multiple cracks upon the dynamic behaviour of beams. In: *Proceedings of the 5th international conference on structural engineering, mechanics and computation*. pp 2199–2204
- Praisach ZI, Gillich GR, Protocsil C, Muntean F (2013) Evaluation of crack depth in beams for known damage location based on vibration modes analysis. *Appl Mech Mater* 430:90–94
- Richardson MH, Mannan MA (1993) Correlating minute structural faults with changes in modal parameters. In: *Proceedings of 11th MAC*. pp 893–898
- Sinou J-J (2009) A review of damage detection and health monitoring of mechanical systems from changes in the measurement of linear and non-linear vibrations”. In: *Mechanical vibrations: measurement, effects and control*. pp 643–702
- Tufoi M, Gillich GR, Praisach ZI, Iancu V, Furdui H (2014) About the influence of temperature changes on the natural frequencies of clamped-clamped euler-bernoulli beams. *Roman J Acoust Vib* 11(2):84–87